

Modelling and Dynamic Study of Cholera Epidemics in Far North Region of Cameroon.

Tchule Nguiwa^{1,1}, Mibailé Justin², Djaouda Moussa³, Gambo Betchewe⁴,
Alidoumouhamadou⁵,

¹Department of Physics, Faculty of Science, University of Maroua, P.O. Box 814, Cameroon.

²Department of Physics, Higher Teachers' Training College, University of Maroua, P.O. Box 55, Cameroon.

³Department of Life and Earth Sciences, Higher Teachers' Training College, University of Maroua, P.O. Box 55, Cameroon.

⁴Department of Physics, Faculty of Science, University of Maroua, P.O. Box 814, Cameroon.

⁵Department of Physics, Faculty of Science, University of Maroua, P.O. Box 814, Cameroon.

Corresponding author: Tchule Nguiwa

ABSTRACT

Cholera continues to emerge in Far North Region of Cameroon and remains an important health challenge. In this work, dynamical system of mathematical model obtained from existing techniques of modelling was studied. The various numerical values obtained such as eigenvalues and basic reproduction number determine the stability of equilibrium points. Cholera epidemiological data given by the Regional Delegation of Health of Far North Region (Cameroon) allowed us to obtain the results using MATLAB software to implement the discretisation of the RungeKutta 4 (RK4) method. The numerical simulations lead us to predict the dynamics of population in the various compartments of the SIR-B cholera transmission model. The results show that when basic reproduction number exceed one, endemic equilibrium is globally asymptotically stable, epidemic becomes permanent. When basic reproduction number is less than one, disease free equilibrium is locally asymptotically stable, epidemic tends to disappear. Overall findings revealed dynamics of propagation of cholera during epidemic period, and so planning the right control actions and strategies could be possible.

KEYWORD: Cholera, *Vibrio cholera*, Epidemiology, Dynamical, Modeling, Stability, Basic Reproduction Number.

Date of Submission: 10-03-2018

Date of acceptance: 26-03-2018

I. INTRODUCTION

Cholera is an acute diarrheal disease caused by ingestion of food or water contaminated with bacterium *Vibrio cholerae* and has a short incubation period of two hours to five days. As well in the world in general and in Africa in particular, cholera remains a redoubtable plague. The first cholera epidemics in Africa were striking with thousands of cases and deaths in few months [1]. The World Health Organization estimates at 1.3 to 4 million cases of cholera per year in the world, including 21 000 to 143 000 deaths [2]. Since 2000, the incidence of cholera has increased steadily, culminating to 317 534 reported cases worldwide, including 7543 deaths with a case-fatality rate of 2.38% in 2010 (The World Health Organization, 2011). Cameroon, just like any other area in the world, faces issues related to frequent Cholera outbreaks throughout the years which led to many deaths. The burden of cholera has increased during the past two decades; the annual number of reported cases (The World Health Organization, 2011) increased, with 4026 cases in 1991, 5796 in 1996, 8005 in 2004 (The World Health Organization, 2004), and 10 759 in 2010 (The World Health Organization, 2010). From 1971 to June 2013, 77152 Cholera cases and 3788 deaths have been reported in Cameroon (Cameroon ministry of the public health). From 1996 to 2011, a total of 24 825 cholera cases were reported in the Cameroon Far North Region

¹Corresponding author.

Email address: tchulealphonse@yahoo.fr (Tchule Nguiwa).

with 1736 death [3]. The epidemics that caused more damage were recorded in 2010 and 2011, represented by figure 1 (Epidemiologic center of the public health of Cameroon Far North Region). In 2014, cholera epidemic was at origin of devastations in 19 health districts of Cameroon Far North Region with 2865 cases and 153 deaths (Regional Delegation of the Ministry of the Public Health of Far North). In spite of provisions taken by the public health, cholera causes enormous damage in human lives and continues to make devastations. The unsafe water, low socio-economic status and poor sanitation are the major transmitting factors of cholera, highlighting other contributing factors like human behavior and practices which are cultural in nature. Then, how can the dynamics of this disease be predicted? in this optics various works was undertaken on mathematical models which make it possible to describe propagation and control of infectious diseases [4,5,6,7,8,9,10,11,12,13,14,15,16,17,18].

Jin Wang and Shu Liao have developed mathematical model for which transmission of the disease is done by two different ways [19]. The susceptible host becomes infected either by direct contact with infectious hosts or via indirect contact with bacteria in contaminated water [19]. Majority of inhabitants of Far North Cameroon are attached to their traditional practices. In addition to the two modes of infections of cholera cited in the model of Jin Wang and Shu Liao, we note a third specific form in Far North Cameroon. The contamination by contact between body of cholera death and a healthy people during funeral rites which lasts a few days before the inhumation. By taking into account a considerable number of infected during traditional practices, it is important to integrate the factor of propagation of cholera by contact between cholera death and susceptible people in model of Jin Wang and Shu Liao. This, in order to appreciate the impact of that contamination rate on the dynamical behavior of the system. Also, a more precise tool with an efficient forecasting of epidemic evolution could be obtained.

Within the framework of our paper, we reconsider the model of Jin Wang and Shu Liao [19] by incorporating the transmission of cholera during funeral (contact between susceptible individual and cholera death) ceremonie. Therefore, this study developed mathematical model of cholera disease that can describe dynamics of cholera transmission in the area of Far North Region of Cameroon.

II. STUDY SITE

The Far North Region is located in the Sudano-Sahelian zone (Fig. 1) and counts about 855398 habitants (Cameroon Regional Delegation of Public Health of Far North) which 70 % of the population lives in rural zone. It is bordered by the North Region to the south, the Republic of Chad to the East, and the Federal Republic of Nigeria to the West. The Far North Region covers an area of 34 263 km⁻¹ subdivided in six administrative Divisions (Diamaré, Mayo-Kani, Mayo-Tsanaga, Mayo-Danay, Mayo-Sava and Logon-and-Chari). Concerning health, that region account 3 regional hospitals, 27 hospitals of districts, 31 health districts, 284 medicals formations and 290 health areas. This region has long and porous border with Chad and Nigeria (10 health district with Chad and 09 health district with Nigeria). It reigns there a tropical climate with a long dry season which lasts 8 to 9 months. Access to clean and safe water or basic sanitary facilities particularly in densely populated areas is poor. Most water used for drinking and domestic activities comes from wells, rivers or community boreholes. Besides the climatic predisposition, it is equally important to note that over 70% of the illnesses in the Far North Region are directly or indirectly associated with poor water supply and sanitation. The endemicity of cholera is caused by weak regards of measurements of hygienes by population, water scarcity in the dry season and water abundance in the raining season, strong defecation out of latrines, human behavior and traditional practices.

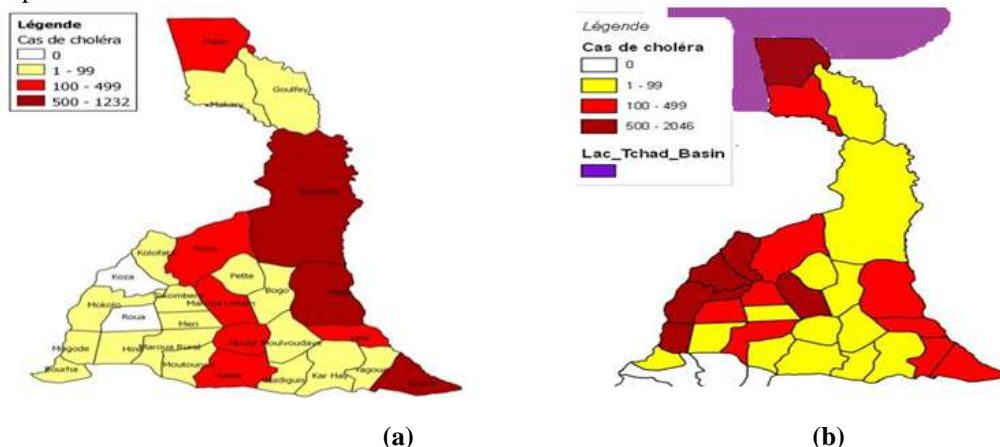


Figure 1: Distribution of the cases of cholera per District of Health (a) in 2010 and (b) 2011 (Cameroon Regional Delegation of Public Health of Far North).

III. MATHEMATICAL MODEL

1.1 Model formulation

The model proposed here is an extension of Jin Wang and Shu Liao model [19], used to describe the cholera epidemics. In our formulation, the cholera infection by handling of cholera deaths during funeral ceremonies was included since this practice could impact seriously the cholera dynamics in Far North region of Cameroon. The total human population is divided into three categories depending on epidemiological status of individuals. Symbols are listed in Table 1 and a diagrammatic representation of the model is shown in Figure 1.

The rectangular boxes represent people: susceptible (S); infectious (I); and recovered (R). The circle represents water reservoir for cholera bacterial agents.

There are several arrows to highlight the different processes below:

- the first compartment is constituted of Susceptible people $S(t)$ who can be infected following contact with individuals infected, contaminated water by choleraic vibrios and cholera deaths,
- the second compartment represents Infected people $I(t)$ who contribute to bacteria shedding,
- the third compartment represents Recovered people $R(t)$.
- The last compartment represents concentration of bacteria $B(t)$ in the environment.

Susceptible people become infected/infectious and they later recover and become immune. Immunity obtained through infection lasts longer than the timeframe studied by the model so the possibility of waning immunity by recovered people is neglected.

In this paper we introduce a mode of contamination by handling the cholera death during funeral ceremonie. The diagram of the model which illustrates the propagation of cholera in Cameroon Far North Region is given by the fig (2)

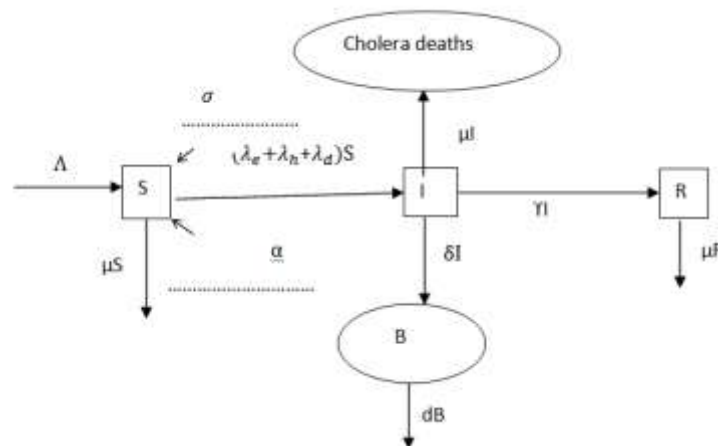


Figure 2: SIR- B Model of cholera

With $\lambda_e = \frac{\alpha B}{\epsilon + B}$, $\lambda_h = \beta I$ and $\lambda_d = \sigma I$. Susceptible individuals acquire cholera infection by ingesting $V. cholerae$ from contaminated water at the rate λ_e , human-to-human transmission at the rate λ_h and cholera death-to-human at the rate λ_d .

Table 1. The descriptive parameters

Parameters	Values
β	The rate of contact between infected individuals and susceptible people(day^{-1}).
α	The rate of exposure to contaminated water (day^{-1}).
σ	Rate of infection due to the cholera death -to-human contact(day^{-1}).
γ	The rate of the cured and immunized individuals (day^{-1}).
δ	The contribution of each infected individual of $V.cholerae$ in the aquatic environment ($\text{cell/ml day-1 person}^{-1}$).
ϵ	Concentration of $V.cholerae$ in the water that yields 50% of chance to be infected (cells/ml).
μ	The natural death rate (day^{-1}).
d	Loss rate of $V.cholerae$ in the aquatic environment (day^{-1}).
Λ	Recruitment rate (day^{-1})

2. 2 Equations System of the model

By considering the above model compartmental, the following differential system is obtained

$$\begin{cases} \frac{dS}{dt} = \Lambda - \mu S - \beta SI - \frac{\alpha BS}{\epsilon + B} - \sigma SI, \\ \frac{dI}{dt} = \beta SI + \frac{\alpha BS}{\epsilon + B} + \sigma SI - (\mu + \gamma)I, \\ \frac{dR}{dt} = \gamma I - \mu R, \\ \frac{dB}{dt} = \delta I - dB, \end{cases} \tag{1}$$

where,

- the first equation of the system characterizes the dynamics of Susceptible people which increase by the rate of new comer Λ . The number of Susceptible people decreases by natural death at the rate μ and contaminated persons determined by expressions $-\beta SI, -\frac{\alpha BS}{\epsilon + B}, -\sigma SI$ which sacking respectively to the infected persons by human-to-human contact, contaminated water and contact with cholera deaths. The contaminated people are transferred to the infected class.
- The second equation of system characterizes dynamics of infected people which decreases by natural death at the rate μ and recovery rate γ .
- The third equation of system translates dynamics of cured persons represented by expression γI and decreases by natural death at the rate μ .

The fourth equation describes variation of *V. cholerae* that grows in the environment by contribution of each infected person at the rate δ and decreases by natural death rate of bacteria d .

The initial conditions are defined as follows

$$S(0) = E_0 \geq 0, I(0) = I_0 \geq 0, R(0) = R_0 \geq 0, B(0) = B_0 \geq 0. \tag{2}$$

Let us pose $f(I, B) = \frac{\alpha B}{\epsilon + B} + (\sigma + \beta)I$ and $g(I, B) = \delta I - dB$, where $f(I, B)$ is the incidence function

determines the rate of new infection and $g(I, B)$ describes the rate of change of choleraic vibrios in environment.

To give a biological meaning to this model, we assume that the two functions f and g satisfy the conditions below for $I \geq 0$ and $B \geq 0$:

- i) $f(0,0) = 0, g(0,0) = 0,$ (3)
- ii) $f(I, B) \geq 0,$ (4)
- iii) $\frac{\partial f(I,B)}{\partial I} \geq 0, \frac{\partial f(I,B)}{\partial B} \geq 0, \frac{\partial g(I,B)}{\partial I} \geq 0, \frac{\partial g(I,B)}{\partial B} \leq 0.$ (5)

We also suppose that the functions $f(I, B)$ and $g(I, B)$ are concaves, i.e.,

$$\text{iv) } \frac{\partial^2 f(I,B)}{\partial I^2} \leq 0, \frac{\partial^2 g(I,B)}{\partial B^2} \leq 0. \tag{6}$$

The condition i) confirms the existence of unique disease free equilibrium (DFE) E_0 of the system (1). The condition ii) translates a positive incidence rate. The first two inequalities of iii) express a higher incidence rate due to the great infection of susceptible people and fast multiplication of choleraic vibrios in environment. In the same way, the third inequality states that increased infection is a consequence of higher growth rate of choleraic vibrios in environment (owing to higher defecation out of the latrines, washings of the clothes and the bodies of the deaths of cholera in environment). The fourth inequality characterizes reduction of the bacteria of environment due to the deaths of choleraic vibrios. Condition iv) is the same assumption condition for nonlinear incidence [20, 21, 22]. About this model, this condition ensures the functions f and h as biologically feasible incidence via a consequence of the effects of saturation. When the number of infected people or concentration of the choleraic vibrios in environment, is very high, many individuals are exposed to the disease agent and the incidence rate will respond more slowly than linearly to the expansion of I and B .

IV. CHOLERA DATA

The weekly cholera epidemiological data used for this work were obtained from the Regional Delegation of Health for the Far North Cameroon. All cholera cases were based on hospital data which were reported to the various health centers and aggregated by health district before being channelled to the regional delegation of Health. The population data includes the total number of people living in each health district during the year of occurrence of various outbreaks. In 2014, The Regional Delegation of Health recorded 2865 cases of cholera with 153 deaths in 19 health Districts. We count 2464 cases of contaminations by infected water, 206 cases by contacts human-to-human and 195 cases by handling of cholera deaths. These data are recapitulated in the following table.

Table 2. Data of cholera epidemic and contaminations sources of Cameroon Far North (Cameroon Far North Regional Delegation of Public Health)

Total population of

Far North Region Cameroon	Contaminations sources	Infected number	Deaths number	Recovered number
3 855 398 infected water	Contamination by	2464	53	2411
Contamination by contact human-to-human	206 75	131		
of cholera deaths	Contamination by handling	195 25	170	

V. BASIC REPRODUCTION NUMBER

The basic reproduction number usually called R_0 is a quantity without dimension which, under certain conditions makes it possible to study the stability of equilibrium points of a dynamic system. This parameter generally used in modeling in ecology, demography and epidemiology is a key and significant concept that the mathematicians brought to the theory epidemics.

The disease free equilibrium (DFE) of system (1) is given by

$E_0 = (S_0, I_0, R_0, B_0) = (A/\mu, 0, 0, 0)$ We evaluate the basic reproduction number to determine the behavior of equilibrium points. The basic reproduction number, R_0 is the average number of secondary infections produced by an infectious individual during his period of infectivity in a population completely consisted of Susceptible [18,13].

We calculate the basic reproduction number by using the next generation operator approach introduced by van den Driessche and Watmough [23]. The new infection generation terms and the remaining transition terms denoted by two matrices F and V are as follows:

$$F = \left(\frac{\partial F_i(x)}{\partial x_j} \right)_{x=x_0} \quad \text{and} \quad V = \left(\frac{\partial V_i(x)}{\partial x_j} \right)_{x=x_0}$$

where $F_i(x)$ is the speed of appearance of new infection in compartment i . They are the new ones infected, obtained by transmission of all left. $V_i(x)$ is the net transfer rate of compartment i , other than infection. On the basis of the system of equations (1) we obtain a new system including the compartments of infectious :

$$\begin{cases} \frac{dI}{dt} = \beta SI + \frac{\alpha BS}{\epsilon + B} + \sigma SI - (\mu + \gamma)I, \\ \frac{dB}{dt} = \delta I - dB. \end{cases} \quad (7)$$

By using the system of equations (7) we can write

$$F_i = \begin{bmatrix} \beta SI + \frac{\alpha BS}{\epsilon + B} + \sigma SI \\ 0 \end{bmatrix} \quad \text{and} \quad V_i = \begin{bmatrix} (\mu + \gamma)I \\ dB \end{bmatrix}.$$

Partial derivatives of F_i and V_i according to I and B at the disease free equilibrium give us;

$$F = \begin{bmatrix} \beta \frac{\Lambda}{\mu} + \sigma \frac{\Lambda}{\mu} & \frac{\alpha \Lambda}{\epsilon \mu} \\ 0 & 0 \end{bmatrix} \quad \text{and} \quad V = \begin{bmatrix} \mu + \gamma & 0 \\ 0 & d \end{bmatrix}$$

It follows that:

$$V^{-1} = \begin{bmatrix} \frac{1}{\mu + \gamma} & 0 \\ 0 & \frac{1}{d} \end{bmatrix}. \quad (8)$$

R_0 is the dominant eigenvalue of the matrix FV^{-1} , where

$$FV^{-1} = \begin{bmatrix} \beta \frac{\Lambda}{\mu(\mu + \gamma)} + \sigma \frac{\Lambda}{\mu(\mu + \gamma)} & \frac{\alpha \Lambda}{\epsilon d \mu} \\ 0 & 0 \end{bmatrix}.$$

The spectral radius for FV^{-1} gives the effective basic reproduction number

$$R_0 = \beta \frac{\Lambda}{\mu(\mu + \gamma)} + \sigma \frac{\Lambda}{\mu(\mu + \gamma)}. \quad (9)$$

R_0 determines the extinction or the persistence of the epidemic as well as the stability of equilibrium points.

Theorem 4.1: The disease-free equilibrium E_0 is locally asymptotically stable when $R_0 < 1$ and unstable when $R_0 > 1$ [6, 24].

Theorem 4.2: The system (1) has a unique endemic equilibrium E^* if $R_0 > 1$ [24].

VI. LINEAR STABILITY ANALYSIS

Here we analyze the existence and local stability of the disease-free and endemic equilibria. Stability means that the trajectories do not change too much under small perturbations.

We linearized the system (1), to analyze the stability of SIR-B model. The corresponding Jacobian matrix is set as

$$J(E_0) = \begin{pmatrix} \mu & -\frac{\beta\Lambda}{\mu} - \frac{\sigma\Lambda}{\mu} & 0 & -\frac{\alpha\Lambda}{\mu\epsilon} \\ 0 & +\frac{\beta\Lambda}{\mu} + \frac{\sigma\Lambda}{\mu} - \mu - \gamma & 0 & \frac{\alpha\Lambda}{\mu\epsilon} \\ 0 & \gamma & -\mu & 0 \\ 0 & \delta & 0 & -d \end{pmatrix} \tag{10}$$

The characteristic polynomial of $J(E_0)$ is

$$\text{Det}(\lambda I - J(E_0)) = (\mu + \lambda)^2 (\lambda^2 + (-\beta + \sigma)S_0 + \mu + \gamma + d)\lambda - S_0 \left(\sigma d + \frac{\alpha\delta}{\epsilon} + d\beta \right) + d(\mu + \gamma).$$

The disease free equilibrium E_0 is asymptotically stable if and only if all roots of the above polynomial have negative real parts.

To solve the equation $\text{Det}(\lambda I - J) = 0$, means that one can write

$$(\mu + \lambda)^2 (\lambda^2 + (-\beta + \sigma)S_0 + \mu + \gamma + d)\lambda - S_0 \left(\sigma d + \frac{\alpha\delta}{\epsilon} + d\beta \right) + d(\mu + \gamma) = 0. \tag{11}$$

We notice that $\lambda = -\mu$ is a negative root. It returns to us to determine the sign of the real part of the various roots of equation (12). This fact we will hold discussions according to the various values of delta.

$$\lambda^2 + (-\beta + \sigma)S_0 + \mu + \gamma + d)\lambda - S_0 \left(\sigma d + \frac{\alpha\delta}{\epsilon} + d\beta \right) + d(\mu + \gamma) = 0, \tag{12}$$

let us evaluate the determinant of equation (12).

$$\Delta = (-\beta + \sigma)S_0 + \mu + \gamma + d)^2 + \frac{4\alpha\delta}{\epsilon} + 4d(-\beta + \sigma)S_0 - (\mu + \gamma).$$

When $\Delta = 0$, we obtain a double solutions

$$\lambda_{1,2} = \frac{(\beta + \sigma)S_0 - \mu - \gamma - d}{2}.$$

by considering $\lambda_{1,2} < 0$, we obtain

$$(\beta + \sigma)S_0 - \mu - \gamma < 0,$$

we end to $R_0 < 1$, then there exist a locally asymptotically stable equilibrium point E_0 . In the contrary case the disease free equilibrium point becomes locally unstable.

When $\Delta < 0$, we obtain

$$(\beta + \sigma)S_0 - \mu - \gamma < 0,$$

thus we arrive at $R_0 < 1$, then The disease-free equilibrium E_0 is locally asymptotically stable.

When $\Delta > 0$, we obtain

$$(\beta + \sigma)S_0 - \mu - \gamma > 0,$$

Then we can write $R_0 > 1$, so that the disease-free equilibrium is unstable. There exist endemic equilibrium point E^* .

Moreover we determine the endemic equilibrium point E^* of the system (1). This point is given by

$$E^* = (S^*, I^*, R^*, B^*) = \left(\frac{\Lambda(d\epsilon + \delta I^*)}{\mu(d\epsilon + \delta I^*) + \alpha\delta I^* + (\beta + \sigma)I^*(d\epsilon + \delta I^*)}, \frac{1}{2} \frac{1}{(\beta + \sigma)(\mu + \gamma)\delta} \left(\left(-\frac{\mu\delta(\mu + \gamma)}{\Lambda} - \frac{\alpha\delta(\mu + \gamma)}{\Lambda} - \frac{d\epsilon(\mu + \gamma)(\beta + \sigma)}{\Lambda} + (\beta + \sigma)\delta + \left(\frac{\mu^2\delta^2(\mu + \gamma)^2}{\Lambda^2} + \frac{2\mu\delta^2\alpha(\mu + \gamma)^2}{\Lambda^2} - \frac{2\mu\delta d\epsilon(\mu + \gamma)^2(\beta + \sigma)}{\Lambda^2} - \frac{2\mu\delta^2(\mu + \gamma)(\beta + \sigma)}{\Lambda} + \frac{(\mu + \gamma)^2\alpha^2\delta^2}{\Lambda^2} + \frac{2\alpha\delta d\epsilon(\mu + \gamma)^2(\beta + \sigma)}{\Lambda^2} + \frac{2\alpha\delta^2(\mu + \gamma)(\beta + \sigma)}{\Lambda} + \frac{d^2\epsilon^2(\mu + \gamma)^2(\beta + \sigma)^2}{\Lambda^2} + \frac{2d\epsilon\delta(\mu + \gamma)(\beta + \sigma)^2}{\Lambda} + (\beta + \sigma)^2\delta^2 \right)^{1/2} \right) \Lambda \right), \frac{\gamma I^*}{\mu}, \frac{\delta I^*}{d} \right).$$

The obtained Jacobian matrix with endemic equilibrium E^* is written as

$$J(E^*) = \begin{pmatrix} -\mu - \beta I^* - \frac{\alpha B^*}{(\epsilon + B^*)} - \sigma I^* & -(\beta + \sigma)S^* & 0 & -\frac{\alpha S^*}{\epsilon + B^*} + S^* \frac{\alpha B^* S^*}{(\epsilon + B^*)^2} \\ \frac{\alpha}{\epsilon + B^*} + \beta I^* + \sigma I^* & (\beta + \sigma)S^* - \mu - \gamma & 0 & \frac{\alpha S^*}{\epsilon + B^*} - S^* \frac{\alpha B^* S^*}{(\epsilon + B^*)^2} \\ 0 & \gamma & -\mu & 0 \\ 0 & \delta & 0 & -d \end{pmatrix}. \tag{14}$$

Let us pose $a_0 = -\mu - \beta I^* - \frac{\alpha B^*}{\epsilon + B^*} - \sigma I^*$, $a_1 = -(\beta + \sigma)S^*$, $a_2 = -\frac{\alpha S^*}{\epsilon + B^*} + S^* \frac{\alpha B^* S^*}{(\epsilon + B^*)^2}$, $a_3 = \frac{\alpha}{\epsilon + B^*} + \beta I^* + \sigma I^*$, $a_4 = (\beta + \sigma)S^* - \mu - \gamma$. The matrix becomes

$$J(E^*) = \begin{pmatrix} a_0 & a_1 & 0 & a_2 \\ a_3 & a_4 & 0 & -a_2 \\ 0 & \gamma & -\mu & 0 \\ 0 & \delta & 0 & -d \end{pmatrix}.$$

The characteristic polynomial of $J(E^*)$ is given by

$$\text{Det}(\lambda I - J(E^*)) = (\mu + \lambda)(c_0\lambda^3 + c_1\lambda^2 + c_2\lambda + c_3). \tag{15}$$

Where

$$c_0 = 1, c_1 = d - a_0 - a_4, c_2 = \delta a_2 + a_4 a_0 - d(a_0 + a_4) - a_1 a_3, c_3 = d a_4 a_0 - \delta a_2(a_0 + a_3) - d a_1 a_3.$$

There exists global stability at the endemic equilibrium point E^* if and only if all roots of the above polynomial have negative real parts. Indeed $\lambda = -\mu$ is a negative solution, we analyze the sign of the other roots. There is a general criterion for determining whether all roots of a polynomial equation have negative real part known as the *Routh–Hurwitz criterion*. This gives conditions on the coefficients of a polynomial equation

$$c_0 \lambda^3 + c_1 \lambda^2 + c_2 \lambda + c_3 = 0.$$

The Routh–Hurwitz conditions are

$$c_1 > 0, c_2 > 0, c_3 > 0, c_2 c_1 > c_0 c_3. \tag{16}$$

The above conditions will be satisfied if

$$d - a_0 - a_4 > 0,$$

$$\delta a_2 + a_4 a_0 - d(a_0 + a_4) - a_1 a_3 > 0, \tag{18}$$

$$d a_4 a_0 - \delta a_2(a_0 + a_3) - d a_1 a_3 > 0, \tag{19}$$

$$(d - a_0 - a_4)(\delta a_2 + a_4 a_0 - d(a_0 + a_4) - a_1 a_3) > d a_4 a_0 - \delta a_2(a_0 + a_3) - d a_1 a_3. \tag{21}$$

We know that

$$a_0 = -\mu - \beta I^* - \frac{\alpha B^*}{(\epsilon + B^*)} - \sigma I^* \leq 0,$$

$$a_1 = -(\beta + \sigma) S^* \leq 0,$$

$$a_3 = \frac{\alpha}{\epsilon + B^*} + \beta I^* + \sigma I^* \geq 0,$$

$$a_4 = (\beta + \sigma) S^* - \frac{f(I^*, B^*) S^*}{I^*} = -\frac{\alpha B^* S^*}{I^* (\epsilon + B^*)} \leq 0.$$

The assumption iv) implies that the surface $f = f(I, B)$ is below its tangent plane at any point $(I^*, B^*) \geq 0$; that is,

$$f(I, B) \leq f(I^*, B^*) + \frac{\partial f}{\partial I}(I^*, B^*)(I - I^*) + \frac{\partial f}{\partial B}(I^*, B^*)(B - B^*), \tag{22}$$

for all $(I, B) \geq 0$. While considering $B = B^*, I = 0$ in equation (22), we obtain

$$0 \leq f(0, B^*) \leq f(I^*, B^*) - \frac{\partial f}{\partial I}(I^*, B^*) I^*$$

$$0 \leq \frac{\alpha B^*}{\epsilon + B^*} + (\sigma + \beta) I^* - (\sigma + \beta) I^* \tag{23}$$

$$0 \leq \frac{\alpha B^*}{\epsilon + B^*}.$$

Let us show inequality (18)

$$\begin{aligned} d - a_0 - a_4 &= d + \mu + f(I^*, B^*) - (\beta + \sigma) S^* + \mu + \gamma \\ &= d + \mu + \frac{\alpha B^*}{\epsilon + B^*} + (\sigma + \beta) I^* - (\beta + \sigma) S^* + \frac{f(I^*, B^*) S^*}{I^*} \\ &= d + \mu + \frac{\alpha B^*}{\epsilon + B^*} + \frac{f(I^*, B^*) S^*}{I^*} \end{aligned}$$

> 0 .

Let us check inequality (19). For that let us evaluate the quantity $\delta a_2 - d(a_0 + a_4)$.

$$\begin{aligned} \delta a_2 - d(a_0 + a_4) &= -\frac{d \alpha B^* S^*}{(\epsilon + B^*) I^*} + \frac{d \alpha B^{*2} S^*}{(\epsilon + B^*)^2 I^*} + d(\mu + (\sigma + \beta) I^*) + \frac{d \alpha B^*}{(\epsilon + B^*)} \\ &- d(\beta + \sigma) S^* + (\beta + \sigma) S^* + \frac{d \alpha B^* S^*}{(\epsilon + B^*) I^*} = \frac{d \alpha B^{*2} S^*}{(\epsilon + B^*)^2 I^*} + d(\mu + (\sigma + \beta) I^*) + \frac{d \alpha B^*}{(\epsilon + B^*)} > 0 \end{aligned}$$

Moreover

$$a_4 a_0 - a_1 a_3 = \frac{\alpha \mu B^* S^*}{(\epsilon + B^*) I^*} + (\mu + \gamma) \left(\frac{\alpha B^*}{(\epsilon + B^*)} + (\sigma + \beta) I^* \right),$$

$$\delta a_2 + a_4 a_0 - d(a_0 + a_4) - a_1 a_3 = \frac{d \alpha B^{*2} S^*}{(\epsilon + B^*)^2 I^*} + d(\mu + (\sigma + \beta) I^*) + \frac{d \alpha B^*}{(\epsilon + B^*)} + \frac{\alpha \mu B^* S^*}{(\epsilon + B^*) I^*} + (\mu + \gamma) \left(\frac{\alpha B^*}{(\epsilon + B^*)} + \sigma + \beta I^* \right) > 0.$$

Let us prove inequality (20). Firstly let us evaluate the quantity

$$\begin{aligned} -\delta a_2(a_0 + a_3) &= -\delta a_2 \left(-\mu - \beta I^* - \frac{\alpha B^*}{(\epsilon + B^*)} - \sigma I^* + \frac{\alpha}{\epsilon + B^*} + \beta I^* + \sigma I^* \right) \\ &= \delta \mu a_2 \end{aligned}$$

$$= -\frac{\alpha \mu d B^* S^*}{(\epsilon + B^*) I^*} + \frac{\alpha \mu d B^{*2} S^*}{(\epsilon + B^*)^2 I^*}.$$

(24)

In continuation, let us calculate

$$da_4a_0 - da_1a_3 = d[(\beta + \sigma)S^* - \mu - \gamma] \left(-\mu - \frac{\alpha B^*}{(\epsilon + B^*)} - (\sigma + \beta)I^* \right) + (\beta + \sigma)S^* \left(\frac{\alpha B^*}{(\epsilon + B^*)} - (\sigma + \beta)I^* \right) = d[\mu(-(\beta + \sigma)S^* + \mu + \gamma) + (\mu + \gamma) \left(\frac{\alpha B^*}{(\epsilon + B^*)} + (\sigma + \beta)I^* \right)] = \frac{\alpha \mu d B^{*2}}{(\epsilon + B^*)} + d(\mu + \gamma) \left(\frac{\alpha B^*}{(\epsilon + B^*)} + (\sigma + \beta)I^* \right) \tag{25}$$

Finally let us add equation (24) to (25) to obtain the following expression

$$-\delta a_2(a_0 + a_3) + da_4a_0 - da_1a_3 = \frac{\alpha \mu d B^{*2} S^*}{(\epsilon + B^*)^2 I^*} + d(\mu + \gamma) \left(\frac{\alpha B^*}{(\epsilon + B^*)} + (\sigma + \beta)I^* \right) > 0.$$

We proceed to show inequality (21)

$$(d + \mu + \frac{\alpha B^*}{\epsilon + B^*} + \frac{\alpha B^* S^*}{(\epsilon + B^*) I^*} + (\sigma + \beta)S^*) \left(\frac{d \alpha B^{*2} S^*}{(\epsilon + B^*)^2 I^*} + d(\mu + (\sigma + \beta)I^*) + \frac{d \alpha B^*}{(\epsilon + B^*)} + \frac{\alpha \mu B^* S^*}{(\epsilon + B^*) I^*} + (\mu + \gamma) \left(\frac{\alpha B^*}{(\epsilon + B^*)} + (\sigma + \beta)I^* \right) \right) = \alpha \mu d B^* 2 S^* \epsilon + B^* 2 I^* + d \mu + \gamma \alpha B^* \epsilon + B^* + \sigma + \beta I^* + d d \alpha B^* 2 S^* \epsilon + B^* 2 I^* + d \mu + \sigma + \beta I^* + d \alpha B^* \epsilon + B^* + \alpha \mu B^* S^* \epsilon + B^* I^* + \mu d \mu + \sigma + \beta I^* + d \alpha B^* \epsilon + B^* + \alpha \mu B^* S^* \epsilon + B^* I^* + \mu + \gamma \alpha B^* \epsilon + B^* + \sigma + \beta I^* + \alpha B^* \epsilon + B^* + \alpha B^* S^* \epsilon + B^* I^* + \sigma + \beta S^* d \alpha B^* 2 S^* \epsilon + B^* 2 I^* + d \mu + \sigma + \beta I^* + d \alpha B^* \epsilon + B^* + \alpha \mu B^* S^* \epsilon + B^* I^* + \mu + \gamma \alpha B^* \epsilon + B^* + \sigma + \beta I^* = c_0 c_3 + d d \alpha B^* 2 S^* \epsilon + B^* 2 I^* + d \mu + \sigma + \beta I^* + d \alpha B^* \epsilon + B^* + \alpha \mu B^* S^* \epsilon + B^* I^* + \mu d \mu + \sigma + \beta I^* + d \alpha B^* \epsilon + B^* + \alpha \mu B^* S^* \epsilon + B^* I^* + \mu + \gamma \alpha B^* \epsilon + B^* + \sigma + \beta I^* + \alpha B^* \epsilon + B^* + \alpha B^* S^* \epsilon + B^* I^* + \sigma + \beta S^* d \alpha B^* 2 S^* \epsilon + B^* 2 I^* + d \mu + \sigma + \beta I^* + d \alpha B^* \epsilon + B^* + \alpha \mu B^* S^* \epsilon + B^* I^* + \mu + \gamma \alpha B^* \epsilon + B^* + \sigma + \beta I^* > c_0 c_3,$$

thus we can write

$$(d - a_0 - a_4)(\delta a_2 + a_4 a_0 - d(a_0 + a_4) - a_1 a_3) > da_4 a_0 - \delta a_2(a_0 + a_3) - da_1 a_3.$$

At the end of calculations carried out above we can conclude that

$$c_1 > 0, c_2 > 0, c_3 > 0, c_2 c_1 > c_0 c_3.$$

Based on the Routh-Hurwitz stability criterion, we can conclude that all roots of a polynomial equation (15) have negative real part. Consequently E^* is an endemic equilibrium point which is locally asymptotically stable. The numerical values of the eigenvalues and of basic reproduction number are calculated in the section 6.

VII. NUMERICAL SIMULATION

The various parameters of follow table 3 have been obtained by means of data given by the Cameroon regional delegation of the public health of Far North.

Table 3. Parameters values used in Numerical simulations.

Parameters	Values
β	0.00894691/day
α	0.10701551/day
σ	0.00846916/day
γ	0.2/day
δ	5.6 (cell/ml day ⁻¹ person ⁻¹)
ϵ	1000000 cell/ml [1, 24]
μ	0.001/day
d	0.033/day [25]
Λ	10/day.

In this section, we present some numerical results of system (1) to justify properties of stability of equilibrium points given by the theorems of section 4. Numerical simulations of the system (1) are carried out by using the parameters values given in Table 3. We calculate initially E_0 and R_0 . By directly computing, we obtain $E_0 = (10000, 0, 0, 0)$ and $R_0 > 1$. The basic reproduction number is greater than one, that supposes the disease free equilibrium E_0 is locally asymptotically unstable and invasion is always possible (see the survey paper by Hethcote) [23]. A unique positive endemic equilibrium E^* of the system (1) exists because $R_0 > 1$. The numerical value of E^* gives $E^* = (10, 50, 9940, 9288)$, then we evaluate the eigenvalues of Jacobian matrix; $\lambda_1 = -0.623381088978441689 + 0.1i$, $\lambda_2 = -0.294246155522720154 + 0.1i$, $\lambda_3 = -0.0300007503988389788 + 0.1i$, $\lambda_4 = -0.010000000000000002 + 0.1i$.

All real parts of the eigenvalues are negatives. We affirm that E^* is locally asymptotically stable. For this case, the disease becomes permanent [24].

➤ Stability of system (1) is described by figure 3: R_0 is lower than one; the disease tends to die out. The curve of susceptible population decreases slightly (this decrease would be explained by a small part of population which becomes infected) simultaneously curve of infected increases slightly and reaches a maximum of 343 individuals at the end of 167 day, then goes down (this regression is due to the cured individuals of cholera and deaths of some) and stabilizes itself. Here stability is justified by the weak variation of infected individuals.

➤ Behaviour of system (1) is described by figure 4: R_0 is greater than one; the disease persists. During the first two weeks the curve of susceptible individuals decreases exponentially from 10000 to 230 individuals before stabilizing itself. During this moment the curve of infected individuals grows quickly and reaches its maximum with 7752 individuals. This great contamination of susceptible population is due to the high rates of contacts of susceptible population with infected individuals, cholera deaths and contaminated water by the choleraic vibrios. The growth of the curve of infected is justified by the new case of infected. After having reached the peak, the growth of infected decrease then is stabilized within 200 days. This stabilization will be explained by the immunity of some and the prudence of others face of plague.

➤ The figure 5 shows a considerable reduction of the number of cases when the rate of contamination by handling body of cholera death is weak. The number of infected individuals varies from 7752 cases with $\sigma = 0.8469 \times 10^{-4}$ (see figure 4) to 5066 cases with $\sigma = 0.8469 \times 10^{-4}$. This variation indicates a significant diminution of 2686 infected cases.

➤ The curves of figure (6a, 6b and 6c) justify stability of equilibrium points.

▪ Firstly, the curve of figure 6a shows us phase portrait of susceptible population according to the infected individuals when $R_0 < 1$, indicating that disease free equilibrium E_0 is globally asymptotically stable and the disease would die out over time.

▪ Secondly, the curve of figure 6b shows us phase portrait of susceptible population according to the infected individuals when $R_0 > 1$, indicating that endemic equilibrium E^* is locally asymptotically stable.

▪ Thirdly, the curves of figure 6c shows us phase portrait of susceptible population according to the infected individuals when $R_0 < 1$ and $R_0 > 1$. We see that all these two orbits converge to the endemic equilibrium, showing the global asymptotic stability of endemic equilibrium.

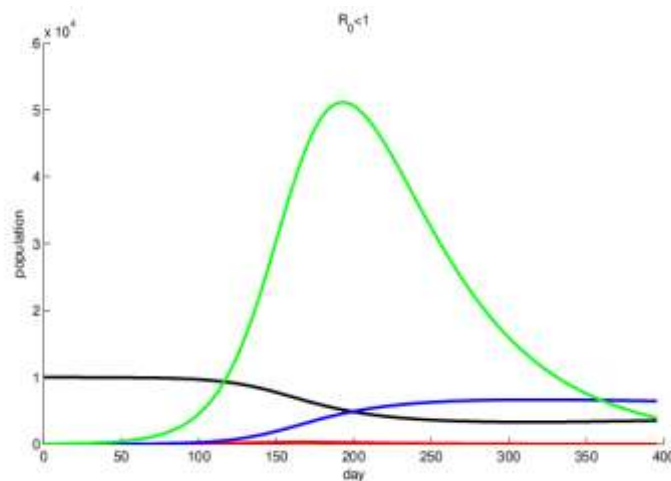


Figure 3: Numerical Simulation of dynamics of human population when $R_0 < 1$. The curves with various colors like black, red, blue and green describe respectively evolutions of susceptible individuals, infected people, recovered people and the choleraic vibrios during the cholera epidemic.

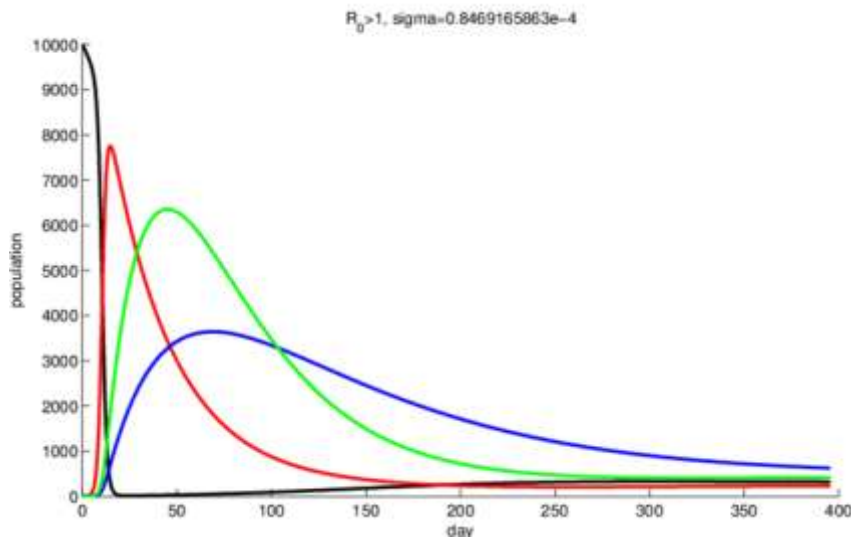


Figure 4: Numerical Simulation of dynamics of human population when $R_0 > 1, \sigma = 0.8469 \times 10^{-4}$. The curves with various colors like black, red, blue and green describe respectively evolutions of susceptible individuals, infected people, recovered people and the choleraic vibrios during the cholera epidemic.

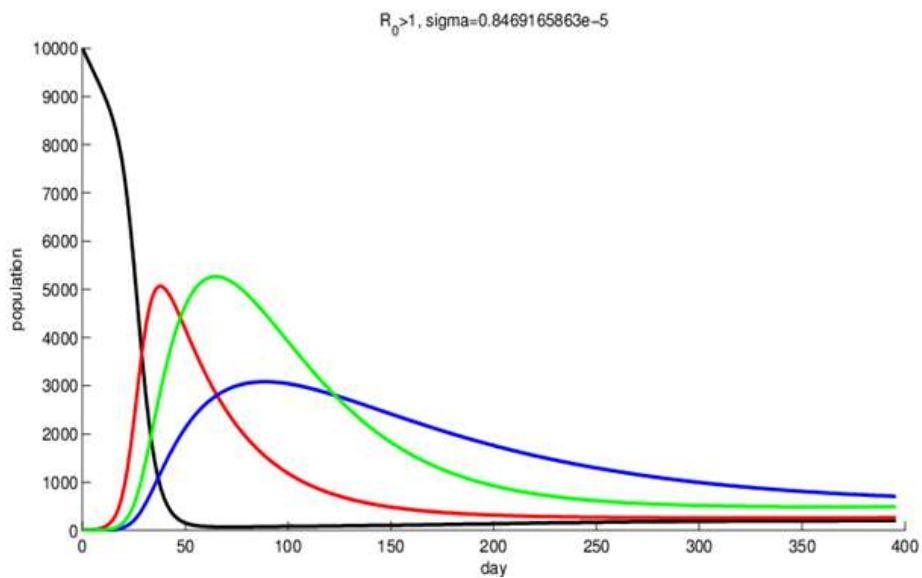


Figure 5: Numerical Simulation of dynamics of human population when $R_0 > 1, \sigma = 0.8469 \times 10^{-5}$. The curves with various colors like black, red, blue and green describe respectively evolutions of susceptible individuals, infected people, recovered people and the choleraic vibrios during the cholera epidemic.

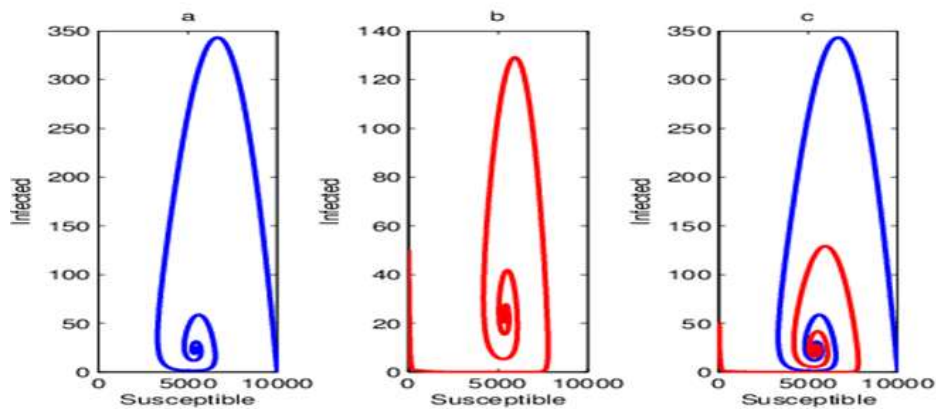


Figure 6: A phase portrait of susceptible as function of infected for the system (1) when $R_0 < 1$ (a); $R_0 > 1$ (b) and $(R_0 < 1, R_0 > 1)$ (c).

VIII. SUMMARY

Propagation of cholera is not only fostered by inter-human contact or contact with contaminated water but also by contact with deaths of cholera. The analyses made at the ends of the numerical simulations allowed us to understand that when $R_0 > 1$, the number of infected people becomes growing during first weeks of epidemic following multiple contacts of susceptible people with infected individuals, cholera death and contaminated water by the choleraic vibrios. After having reached peak, this number decreases before stabilizing itself: the epidemic becomes permanent. By considering $R_0 < 1$, the numbers of the infected people remain weak: Epidemic tends to disappear. We also underline possibility to reduce the number of infected cases by avoiding practices of traditional rites that support contaminations by handling body of cholera death. This work clarifies us on evolution of cholera during epidemic period in Far North Region of Cameroon. Thus, this produced work will allow the Cameroon public health ministry to effectively conceive fast strategies of interventions to extinguish this epidemic.

ACKNOWLEDGEMENTS

The research described in this paper was initiated at Clinic on Dynamical Approaches to Infectious Disease Data. Authors are very grateful to the organizers of ICI3D Program - Emerging Pathogens Institute - University of Florida

REFERENCES

- [1]. Emch, M., Feldacker, C., Islam, M. S., and Ali, M.: Seasonality of cholera from 1974 to 2005: a review of global patterns, *Int. J. Health Geogr.*, 20:7-31, 2008.
- [2]. OMS, "Choléra 2014", *Relevé épidémiologique hebdomadaire*, 40 :517-544, 2015.
- [3]. Arabi, Xiao, Taiwe - Liang, Cholera Incidence in Cameroon's Far North Region *African Journal of Social Sciences* 5: 9-10, 2014.
- [4]. Capasso V, Pavari-Fontana SL: A mathematical model for the cholera epidemic in the europeanmediterranean region. *Rev Epidémet Santé Pub*, 27:121-132, 1979.
- [5]. P. van den Driessche, J. Watmough, Reproduction numbers and subthreshold endemic equilibria for compartmental models of disease transmission, *Math. Biosc.*, 180: 29-48, 2002.
- [6]. Castillo-Chaves, C., and Song, B., "Dynamical Models of Tuberculosis and Their Applications," *Mathematical Biosciences and Engineering*, 1:361-404, 2004.
- [7]. C. T. Codeco, Endemic and epidemic dynamics of cholera: the role of the aquatic reservoir, *BMC Infect Dis.*, 2001.
- [8]. Pascual, M., Bouma, M.J., Dobson, A.P. Cholera and climate: revisiting the quantitative evidence, *Microb. Infect*, 4: 237 – 245, 2002.
- [9]. G.C. De Magny et al, modeling environmental impacts of plankton reservoirs on cholera population dynamics *ESAIM : PROCEEDINGS*, 14:156-173, 2005.
- [10]. P.T. Jianjun, S. Liao, J. Wang, analyzing the infection dynamics and control strategies of cholera, *discrete and continuous dynamical systems*, 1:747-757, 2013.
- [11]. PrabirPanja, Shyamal Kumar Mondal, A mathematical study on the spread of Cholera, *South Asian Journal of Mathematics*, 4: 69-84, 2014.
- [12]. J.P. Tian and J. Wang, Global stability for cholera epidemic models, *Mathematical Biosciences*, 232:31-41, 2011.
- [13]. M. Ghosh, P. Chandra, P. Sinha and J. B. Shukla, Modeling the spread of carrierdependent infectious diseases with environmental effect, *Applied Mathematics and Computation*, 152: 385-402, 2004.
- [14]. D.M. Hartley, J.G. Morris and D.L. Smith, Hyperinfectivity: a critical element in the ability of *V. cholerae* to cause epidemics? *PLoS Medicine*, 3: 63-69, 2006.
- [15]. A.A. King, E.L. Lonides, M. Pascual and M.J. Bouma, Inapparent infections and cholera dynamics, *Nature*, 454:877-881, 2008.
- [16]. Z. Mukandavire, S. Liao, J. Wang and H. Ga, Estimating the basic reproductive number for the 2008-2009 cholera outbreak in Zimbabwe, 2010.
- [17]. J.H. Tien and D.J.D. Earn, Multiple transmission pathways and disease dynamics in a waterborne pathogen model, *Bulletin of Mathematical Biology*, 72:1502-1533, 2010.
- [18]. O. Diekmann, J.A.P. Heesterbeek, and J.A.J. Metz, On the definition and the computation of the basic reproduction ratio R_0 in models for infectious diseases in heterogeneous population, *J. Math. Biol.*, 28: 365-382, 1990.
- [19]. Jin Wang and Shu Liao. A generalized cholera model and epidemic-endemic analysis, *Journal of Biological Dynamics*, 6: 568-589, 2012.
- [20]. H. W. Hethcote, The mathematics of infectious diseases, *SIAM Rev*, 42: 599- 653, 2000.
- [21]. A. Korobeinikov and P.K. Maini, Non-linear incidence and stability of infectious disease models, *Math. Med. Biol.*, 22:113-128, 2005.
- [22]. S.M. Moghadas and A.B. Gumel, Global stability of a two-stage epidemic model with generalized non-linear incidence, *Math. Comput. Simul.*, 60:107-118, 2002.
- [23]. Hethcote H W. The mathematics of infectious diseases, *SIAM Rev*, 42: 599- 653, 2000.
- [24]. R. P. Sanches, C. P. Ferreira, R. A. Kraenkel, The Role of Immunity and Seasonality in Cholera Epidemics, *Bull. Math.Biol.*, 73: 2916-2931, 2011.
- [25]. Hartley, D. M., Morris J. G., and Smith, D. L., "Hiperinfectivity : A Critical Element in the Ability of *V. Cholerae* to Cause Epidemics?," *PLoS Med*, 3:63-68, 2006.

Tchule Nguwa " Modelling and Dynamic Study of Cholera Epidemics in Far North Region of Cameroon." *International Journal of Computational Engineering Research (IJCER)*, vol. 08, no. 03, 2018, pp. 06-16.